

FINITE ELEMENT ANALYSIS OF MULTI-STAGE DEEP DRAWING FOR FORMING DEEP RECTANGULAR CASE WITH HIGH ASPECT RATIO

SHOHEI KAJIKAWA^{*}, TOMOYA TAKASAN[†], TAKASHI KUBOKI[†],
KENJI TAMAOKI^{††}, KATSUYUKI ONISHI^{†††},
AKIRA GUNJI^{†††} AND AKIRA YAMAUCHI^{†††}

^{*} Department of Mechanical and Intelligent Systems Engineering
The University of Electro-Communications
1-5-1 Chofu Gaoka, Chofu-shi, Tokyo, 182-8585, Japan
E-mail: s.kajikawa@uec.ac.jp - Web page: <http://www.uec.ac.jp/eng/>

[†] Department of Mechanical and Intelligent Systems Engineering
The University of Electro-Communications
1-5-1 Chofu Gaoka, Chofu-shi, Tokyo, 182-8585, Japan

^{††} Tokyo Metropolitan Industrial Technology Research Institute
1-20-20 Minamikamata, Ota-ku, Tokyo, 144-0035, Japan
Web page: <http://www.iri-tokyo.jp/>

^{†††} Yamauchi Engineering Co., Ltd.
2327-2 Tana, Chuo-ku, Sagami-hara-shi, Kanagawa, 252-0244, Japan
Web page: <http://yama-eng.com/>

Key words: Deep Drawing, Rectangular Case, Sheet Metal, Aluminum, FEM.

Abstract. This paper presents investigations on multi-stage deep drawing for producing a flat and deep rectangular case, of which a cross section is high aspect ratio. Effects of a blank shape on a formability was investigated for preventing a local thinning and a large ear by using the finite element method (FEM) analysis. The multi-stage deep drawing was composed of four stages. The first and the second stage were deep drawing and redrawing process, and the third and the fourth stage were ironing process. The blank was the rectangle with the elliptic corners, and the longitudinal length l_b and the elliptic corner length r_{1b} was changed. The local thinning and the ear were reduced by appropriately setting l_b and r_{1b} . In addition, the effect of the aspect ratio on the formability was small. Therefore, the optimized blank could be applied for forming the flat and deep rectangular case with various aspect ratio.

1 INTRODUCTION

Production of the electric vehicle (EV) is drastically expanding for achieving sustainable developments, and manufacturing technologies of various components of the EV are important. A lithium-ion battery case is one of the specific components of the EV. The battery case is a

flat and deep rectangular container, which has a cross-sectional shape with high aspect ratio as shown in Figure 1(a), because this shape is appropriate for a heat dissipation and a space saving. High dimensional accuracy is required in order to apply this container to the battery case. In addition, the aspect ratio of the cross-section should be increased for large capacity. The battery case was generally produced by multi-stage deep drawing, impact extrusion and welding. The impact extrusion is effective for mass production because the processing time is very short [1]. However, it is difficult to precisely control the wall thickness. The deep case without any defects is easily produced by the sheet metal bending and welding [2], while it is difficult to secure stable welding strength. Therefore, the multi-stage deep drawing is appropriate for producing the battery case because it realizes high dimensional accuracy and lower processing load compared to the impact extrusion, and mass production compared to the sheet metal bending and welding.

Some forming defects, such as a crack, a wrinkle and ears, should be prevented on the deep drawing. There are many research works about deep drawing, and process parameters had been optimized [3]. For example, the wrinkles and the cracks could be prevented by appropriately controlling the blank holder force [4,5]. The blank shape is also important for preventing the crack and the ear, and it should be considered depending on the cup shape [6]. However, there are few investigations for the multi-stage deep drawing of the flat rectangular cup, which is used for the battery case.

The deformation style on forming the flat rectangular case is considered to be different from that on forming the cylinder or the square cup. It is a combination of the bending and the deep drawing as shown in Figure 1 (b). The middle portion in the longitudinal direction is simple bending and unbending, while the deformation style at the edge portion is considered to be the radial stretching with the hoop shrinkage. In the range between the middle and the edge, it is considered that the deformation style change from the bending to the deep drawing. For forming the flat rectangular cup without any defects, the deformation behaviour should be understood, and optimum forming parameters should be investigated. In particular, the blank shape is important for preventing the crack and reducing the ear.

In this study, the effect of the blank shape on the formability was investigated by using the finite element method (FEM) analysis on the multi-stage deep drawing of the flat and deep

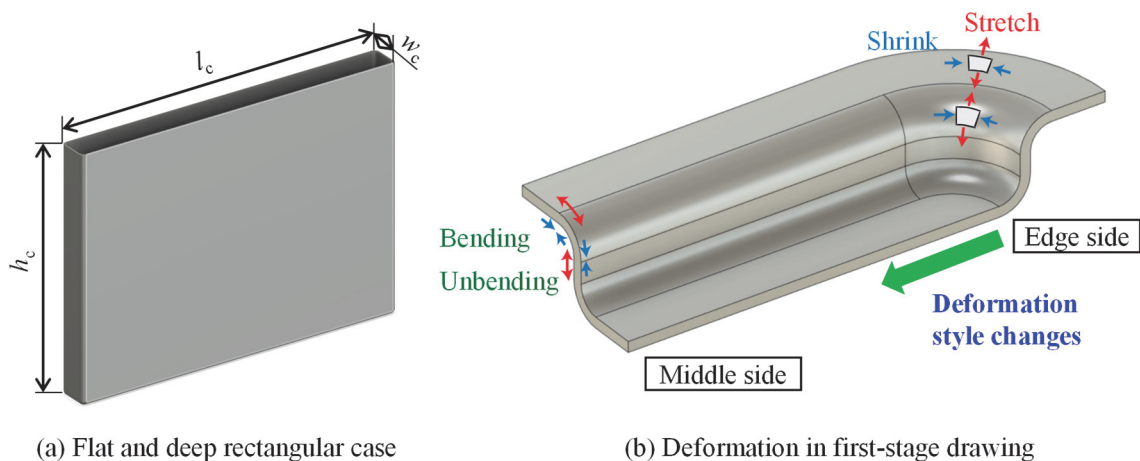


Figure 1: Schematic diagram of forming flat and deep rectangular case

rectangular case. The thickness distribution and the ear height were evaluated for each drawing stage. After optimization of the blank shape, the effect of the aspect ratio was investigated for clarifying the range in the application of the optimized blank shape.

2 METHOD

Figure 2 shows an analysis model of four-stage deep drawing for FEM. An elastic-plastic analysis was carried out by using a commercial code “ELFEN” which was developed by Rockfield Software Limited, Swansea. The model was three dimensional, and an explicit scheme was adopted. The model was half by considering symmetry of the blank and the rectangular case for shortening the analysis time.

Figure 3 and Table 1 show the blank shape and conditions for forming the case of which the dimension is $l_c \times w_c \times h_c$ as shown in Figure 1 (a). The blank was elastic-plastic, and the von Mises yield criterion was adopted. The element shape was four-node tetrahedral. Adaptive remeshing scheme was adopted for preventing distortion of the element. A grid, of which a size was 2×2 mm, was set to the blank surface in order to see the flow pattern on the analysis with the adaptive remeshing. The blank shape was determined by the length l_b , w_b , and the corner length r_{lb} , r_{wb} . The blank shape was changed variously by changing l_b and w_b , while l_{yb} and l_{ryb} were constant. l_b and w_b was determined as follow,

$$l_b = l_c + 2ah_c \quad (1)$$

$$r_{lb} = \beta r_{wb} \quad (2)$$

where α and β are length factors for controlling l_b and w_b . If α is 1.0, the distance between the blank end and the die hole in the longitudinal direction was the same as that in the width direction. The blank corner shape was a circular arc in a case of $\alpha=1.0$, otherwise it was an elliptic arc.

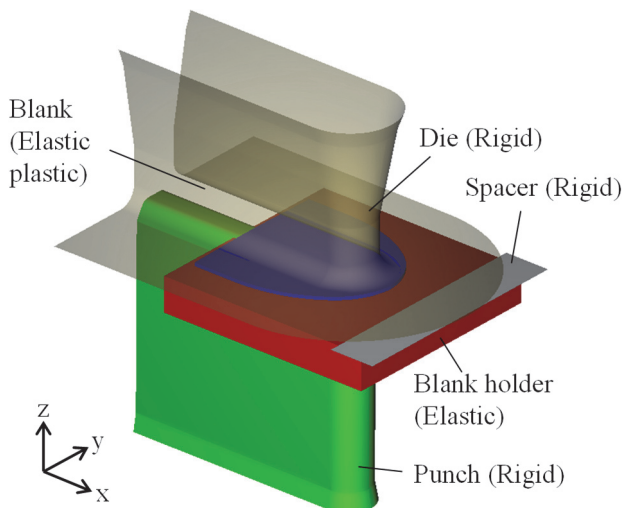


Figure 2: Schematic diagram of analysis model (First stage)

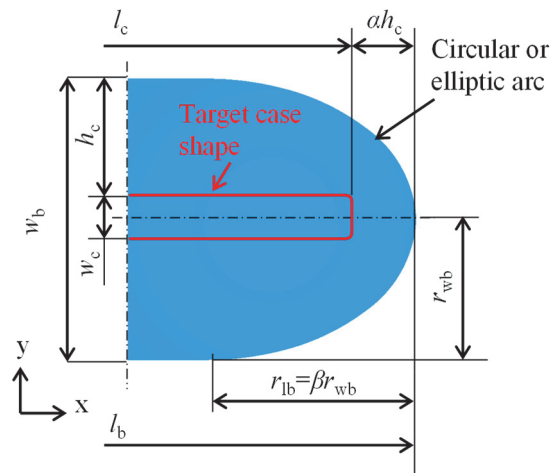


Figure 3: Blank shape

Table 1: Conditions for blank for forming case which dimension is $l_c \times w_c \times h_c$

Material	Aluminum alloy 3003 (Elastic plastic)	
Swift's equation	$\sigma = 218(\epsilon_p + 0.0026)^{0.285}$	
Length	l_b [mm]	$l_c + 2ah_c$
	w_b [mm]	$w_c + 2h_c$
Corner length	r_{lb} [mm]	βr_{wb}
	r_{wb} [mm]	$w_c/2 + h_c$
Thickness t_0 [mm]	2	
Average length of element edge [mm]	1 stage	0.60~0.70
	2 stage	0.60~0.70
	3 stage	0.45~0.55
	4 stage	0.25~0.35

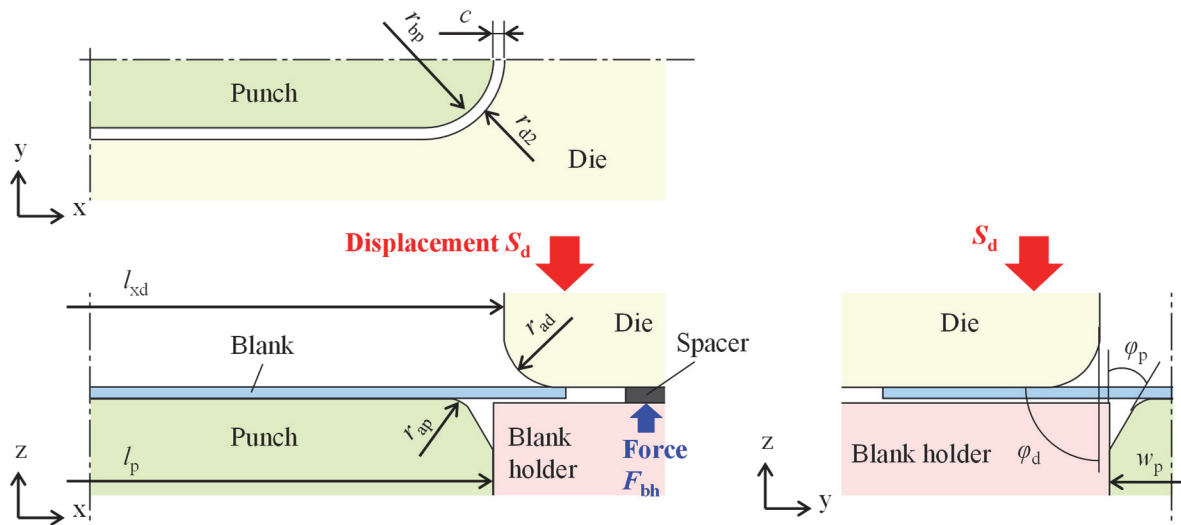


Figure 4: Schematic diagram of cross section of tools

Figure 4 and Table 2 show the schematic of the detailed tool shapes and dimensions, and Table 3 shows the working conditions. The punch and the die were rectangular shape which corners were rounded. The blank was formed by moving the die, while the punch was fixed. The force F_{bh} was loaded to the blank holder, and a minimum gap between the die and the blank holder was t_s by setting the spacer which thickness was t_s . Figure 5 shows the cross sectional views for each stage. The blank was drawn and redrawn in the first and the second stages. After the second stage, the side wall was ironed at the third and the fourth stages.

Thickness t and height h of the formed case were evaluated. Ear height h_{ear} was defined as the following equation

$$h_{ear} = h_{max} - h_{min} \quad (3)$$

where h_{max} and h_{min} are maximum and minimum height of the case. Short h_{ear} leads to the scrap reduction.

Table 2: Tool dimensions for forming case which dimension is $l_c \times w_c \times h_c$

		Stage number			
		1	2	3	4
Die	Length l_d [mm]	$l_c+16.5$	$l_c+1.3t_0$	$l_c+0.4t_0$	l_c
	Width w_d [mm]	$w_c+16.5$	$w_c+1.3t_0$	$w_c+0.4t_0$	w_c
	Corner radius r_{ad} [mm]	10	10	10	10
	radius r_{bd} [mm]	14.9	4.3	2.5	2.0
Punch	Length l_p [mm]	$l_c+16.5-2t_0$	$l_c-0.7t_0$	$l_c-0.7t_0$	$l_c-0.7t_0$
	Width w_p [mm]	$w_c+16.5-2c_1$	$w_c-0.7t_0$	$w_c-0.7t_0$	$w_c-0.7t_0$
	Corner radius r_{ap} [mm]	5	1.7	1.7	1.7
	radius r_{bp} [mm]	12.9	2.3	2.3	2.3
Clearance c [mm]		t_0	t_0	$0.55t_0$	$0.35t_0$
Spacer thickness t_s [mm]		$t_0+0.5$			

Table 3: Working conditions

Blank holder force F_{bh} [N]	2000	
Friction coefficient	Blank-Punch μ_p	0.22
	Blank-Die μ_p	0.05
	Blank-Blank holder μ_{hf}	0.05

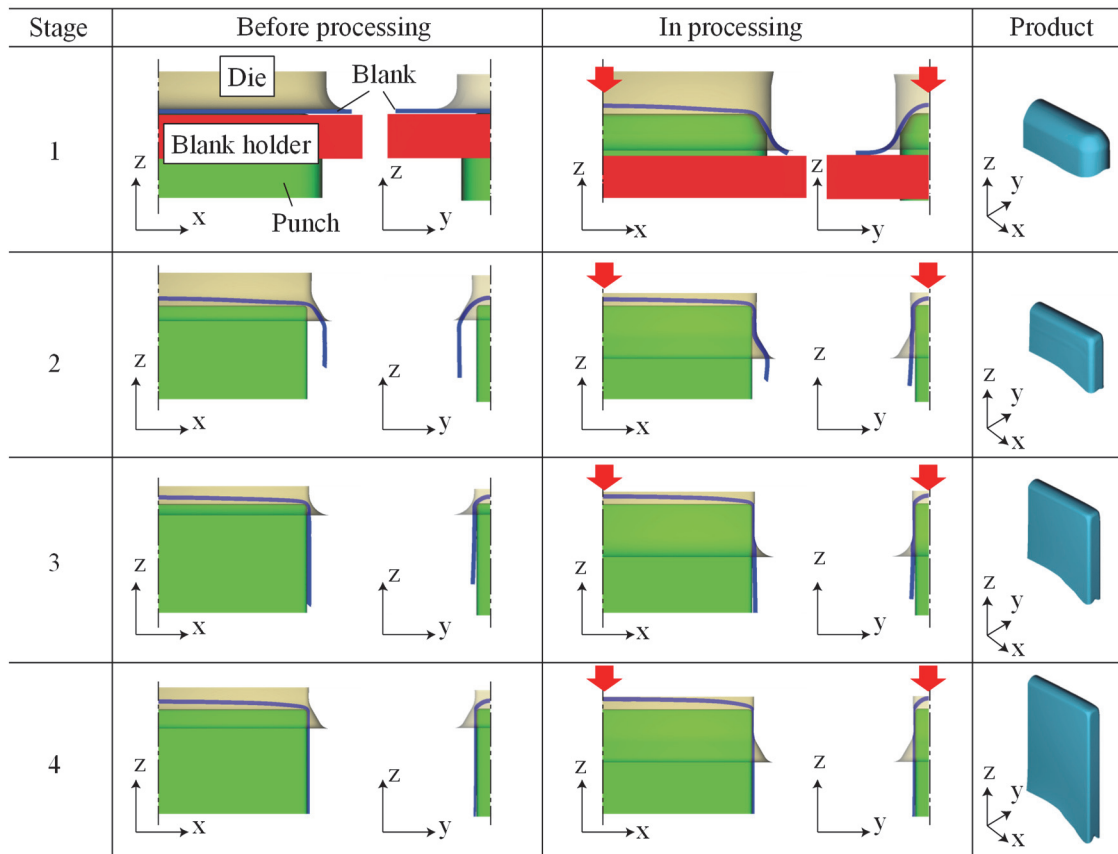


Figure 5: Cross sectional view during process

3 RESULT AND DISCUSSION

3.1 Effect of blank length

The effects of the blank length l_b on the formability in the first and the second stage was investigated. Table 4 and Figure 6 shows the conditions and a quarter of the blank shapes with the die shape for this investigation. The blank corner length r_{1b} was constant to 43 mm, of which the length factor β was 1.0. Figure 7 shows the deformation of the grid after the first and the second stage drawing when l_b was 176 mm. The grid did not deform at the middle side in the longitudinal direction. This suggests that the wall deformation was the bending and the unbending by passing on the die corner, and then the wall was not stretched at the middle portion. On the other hand, the grid largely stretched in the height direction, while it shrank in the hoop direction at the edge side. Therefore, the edge side height was higher than the middle side height. The deformation style at the edge side is similar to that of the deep drawing for

Table 4: Conditions for investigation on effect of blank length

blank length		
Target	Length l_c [mm]	137
case	Width w_c [mm]	13.3
shape	Height h_c [mm]	36.35
Blank	Length l_b [mm]	159 ($\alpha=0.30$), 176 ($\alpha=0.54$), 185 ($\alpha=0.66$), 193 ($\alpha=0.77$), 202 ($\alpha=0.89$), 210 ($\alpha=1.00$)
	Width w_b [mm]	86
	Corner length	r_{1b} [mm] 43 ($\beta=1.00$) r_{wb} [mm] 43

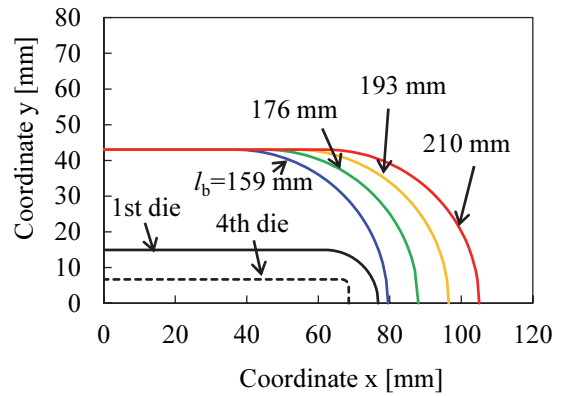


Figure 6: Effect of blank length l_b on blank shape ($\beta=1.00$)

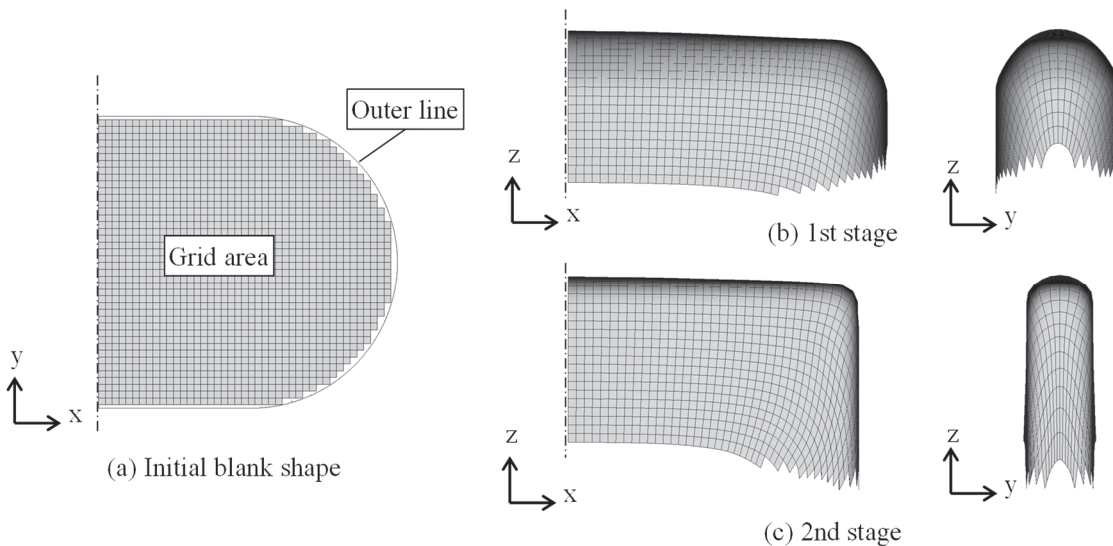


Figure 7: Deformation of grid in first and second stage ($\alpha=0.54$, $\beta=1.00$)

forming the cylindrical or the square cup. From this result, it was confirmed that the deformation style on forming the flat rectangular case is the combination of the bending and the deep drawing.

Figure 8 shows the appearances of the cases with the distribution of the thickness t after the first and the second stage drawing. The distribution of t changed by the blank length l_b , and a local thinning occurred at the punch shoulder at the edge side. In addition, the height h at the edge side changed with the change of l_b . In the case that l_b was too short such as $l_b=159$ and 168 mm, a folding occurred in the second stage, because h was too low at the edge side after the first stage as shown in Figure 8 (a). On the other hand, h at the edge side increased with an increase in l_b .

Figure 9 shows the effect of the blank length l_b on the minimum thickness t_{\min} . t_{\min} decreased with the increase in l_b in the first stage. This is because the drawing load was high due to large flange shrinkage in the hoop direction at the edge side as shown in Figure 7, which led to the local thinning at the punch shoulder. This local thinning of the first stage affected the thickness distribution of the second stage. In the second stage, t_{\min} also decreased with the increase in l_b as shown in Figure 9, and the thin area was large on the side wall as shown in Figure 8 (d).

Figure 10 shows the effect of the blank length l_b on the ear height h_{ear} . In the first stage, h_{ear} changed with the edge side height, while the middle side height was almost constant. When l_b was 159~176 mm, the edge side height was smaller than the middle side height. Then, h_{ear} decreased with the increase in l_b as the edge side height increased to the middle side height. On the other hand, the edge side height was larger than the middle side height when l_b was 185~210 mm. Then, h_{ear} increased with the increase in l_b , because the edge side height increased although the middle side height was constant. In the second stage, the folding occurred as the edge side height was too low under the condition of $l_b=159$ and 168 mm. When l_b was larger than or equal to 176 mm, the edge side height got larger due to the radial stretching with the shrinkage in the hoop direction, and then h_{ear} increased with an increase in l_b . From the above result, the appropriate blank length l_b was 176 mm, which α was 0.54 , for preventing the folding, the local

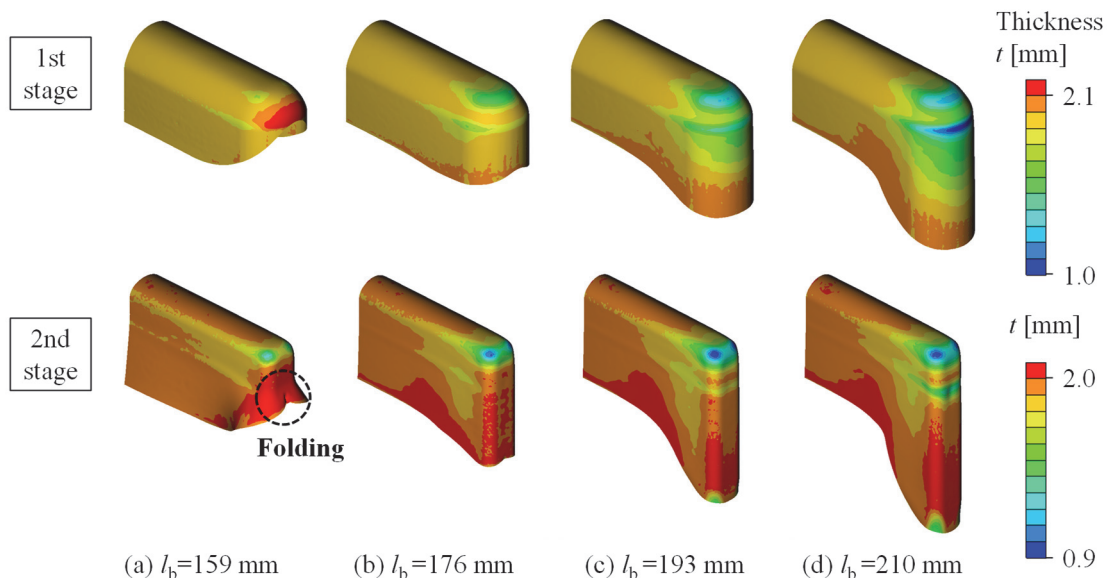


Figure 8: Case appearances with thickness t distribution for each blank length l_b ($\beta=1.00$)

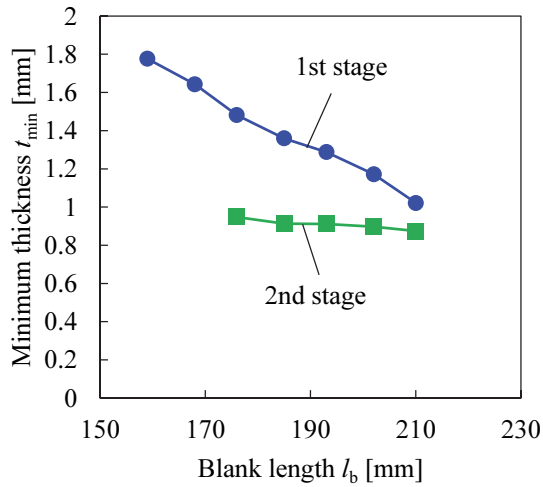


Figure 9: Effect of blank length l_b on minimum thickness t_{min} after first and second stage ($\beta=1.00$)

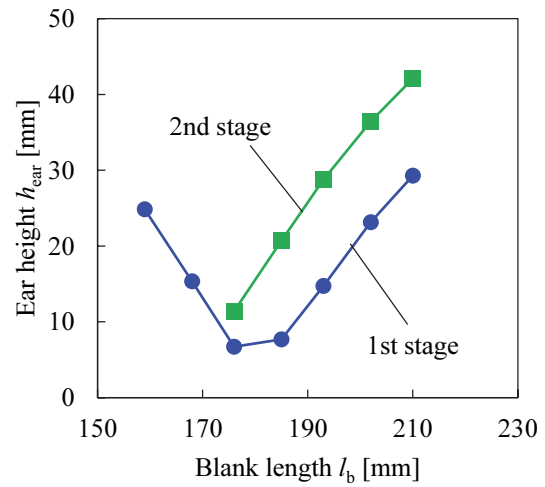


Figure 10: Effect of blank length l_b on ear height h_{ear} of case after first and second stage ($\beta=1.00$)

thinning and the ear. However, the blank volume at the edge side should be decreased more for reducing the ear, because the edge side height was larger than the middle side height in the case that l_b was 176 mm as shown in Figure 8 (b).

3.2 Effect of blank corner length

The effects of the blank corner length r_{1b} on the formability was investigated. Table 5 shows the conditions on this investigation. The blank length l_b was constant of 176 mm (Length factor $\alpha=0.54$), which was optimum when the blank corner was the circular arc (Length factor $\beta=1.0$). Figure 11 shows the blank shapes with the die shape in this investigation. The blank corner shape was the elliptic arc, and the blank volume decreases with the increase in r_{1b} .

Figure 12 shows the appearances of the cases with the distribution of the thickness t after the first, the second and the fourth stage. The distribution of t changed by the blank corner length r_{1b} . The area of the local thinning, which occurred at the edge side punch shoulder, decreased with the increase in r_{1b} after the first stage. In addition, the edge side height decreased with the increase in r_{1b} after the first stage, which lead the difference of the ear shape after the fourth stage.

Figure 13 shows the effect of the blank corner length r_{1b} on the minimum thickness t_{min} . t_{min} slightly increased with the increase in r_{1b} at the first and the second stage, but these changes were small. On the other hand, the ear height h_{ear} drastically changed by r_{1b} as shown in Figure 14. After the first stage, h_{ear} was minimum when r_{1b} was 54 mm. On the other hand, the optimum r_{1b} for preventing the ear changed to 64 mm after the second stage, because h_{ear} increased with the edge side height increasing due to the radial stretching with the hoop shrinkage by the redrawing. As for the third and the fourth stages, which were ironing process, h_{ear} increases in each stage, while the optimum r_{1b} was constant of 64 mm. Therefore, it was important to prevent the ear occurrence at the drawing and redrawing process before the ironing process.

Table 5: Conditions for investigation on effect of blank corner length

Target	Length l_c [mm]	137
case	Width w_c [mm]	13.3
shape	Height h_c [mm]	36.35
Blank	Length l_b [mm]	176 ($\alpha=0.54$)
	Width w_b [mm]	86
Corner length	r_{lb} [mm]	43 ($\beta=1.00$),
		54 ($\beta=1.26$),
		64 ($\beta=1.49$),
		74 ($\beta=1.72$),
		84 ($\beta=1.95$)
	r_{wb} [mm]	43

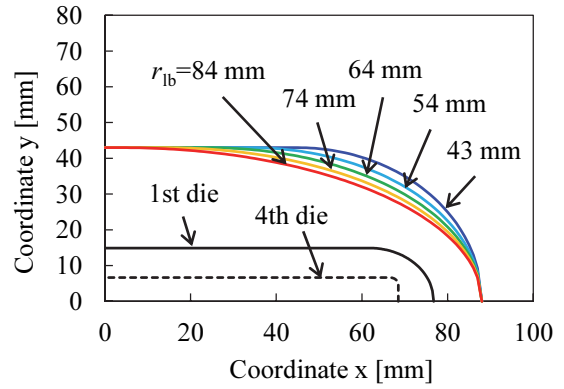


Figure 11: Effect of blank length r_{lb} on blank shape ($\alpha=0.54$)

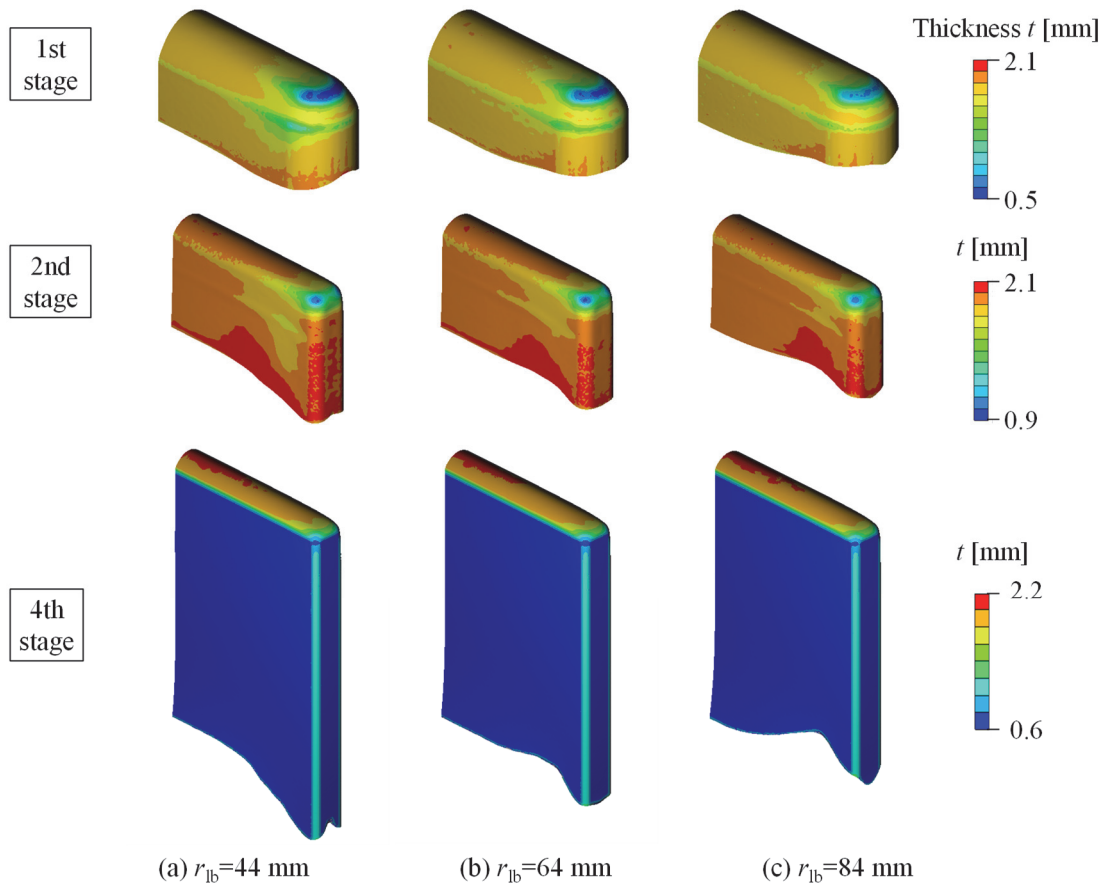


Figure 12: Case appearances with thickness distribution for each blank corner length r_{lb} ($\alpha=0.54$)

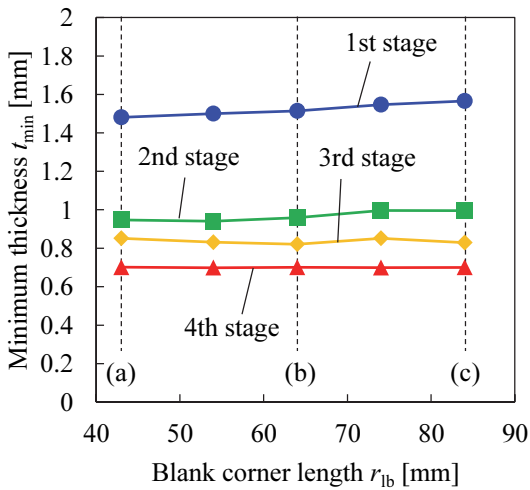


Figure 13: Effect of blank corner length r_{lb} on minimum thickness t_{\min} after each stage ($\alpha=0.54$)

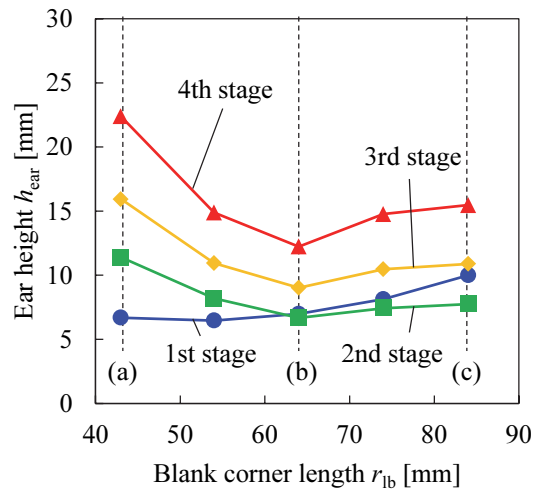


Figure 14: Effect of blank corner length r_{lb} on ear height h_{ear} after each stage ($\alpha=0.54$)

3.3 Effect of aspect ratio

The effect of the aspect ratio l_c/w_c was investigated for clarifying the range in the application of the optimized blank shape, which was determined by length factor α and β . Table 6 shows the conditions on this investigation. l_c/w_c was changed by changing the target length l_c of the case while target width w_c was constant. The blank length l_b was changed along with l_c/w_c , while the length factors α and β were constant. α and β were 0.54 and 1.72 based on the previous investigations. The blank shape was ellipse under the condition of $l_c=89$ mm, and it was rectangle with elliptic corner under the condition that l_c was 103~274 mm.

Figure 15 shows the change of the case appearances when the aspect ratio l_c/w_c was varied. The effect of l_c/w_c on the thickness t distribution and the ear shape was very small. The effect of on the minimum thickness t_{\min} and the ear height h_{ear} was also small as shown in Figure 16 and 17. From this result, the optimized length factor α and β could be applied to forming the flat rectangular case with the cross section which aspect ratio is extremely high. On the other hand, the optimized α and β is not applied to the condition that l_c/w_c is lower than 6.7, because the blank length is shorter than the length of double length of r_{lb} . Therefore, a further investigation is needed if the flat rectangular case, which l_c/w_c is lower than 6.7, is needed.

Table 6: Conditions for investigation on effect of aspect ratio

Target case shape	Length l_c [mm]	89, 103, 137, 172, 206, 240, 274
	Width w_c [mm]	13.3
	Height h_c [mm]	36.35
Blank	Length l_b [mm]	128, 142, 176, 211, 245, 279, 313 ($\alpha=0.54$)
	Width w_b [mm]	86
	Corner length r_{lb} [mm]	64 ($\beta=1.49$)
	r_{wb} [mm]	43

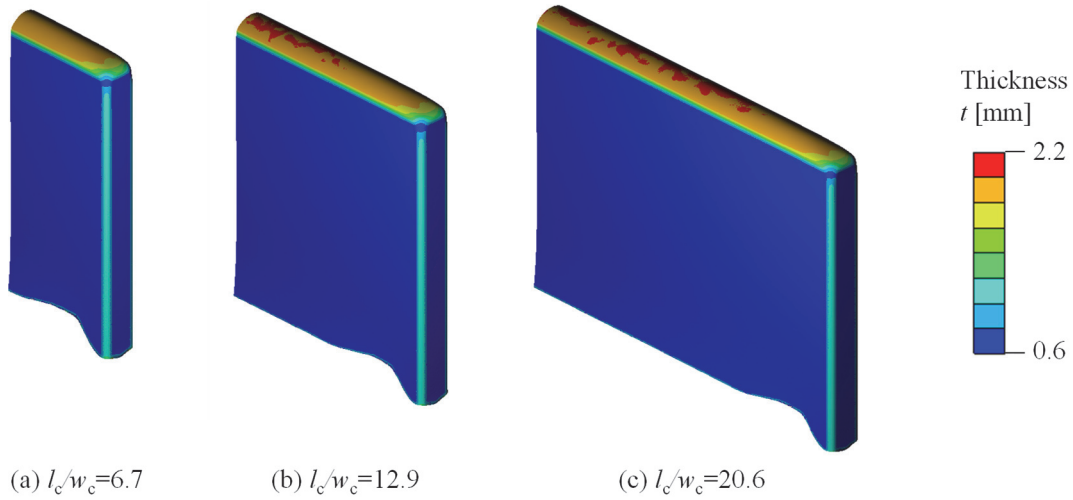


Figure 15: Case appearances after 4th stage with thickness t distribution for each aspect ratio l_c/w_c ($\alpha=0.54, \beta=1.72$)

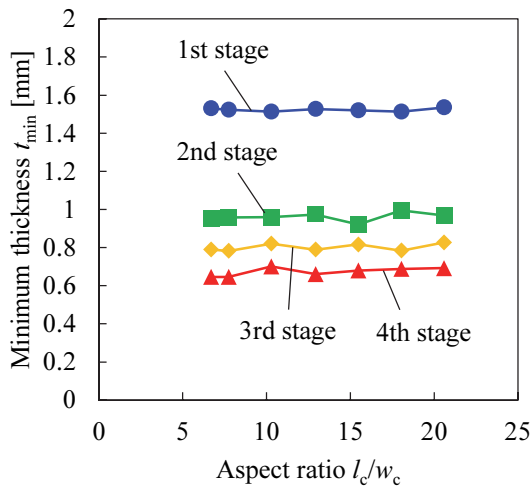


Figure 16: Effect of aspect ratio l_c/w_c on minimum thickness t_{\min} after each stage ($\alpha=0.54, \beta=1.72$)

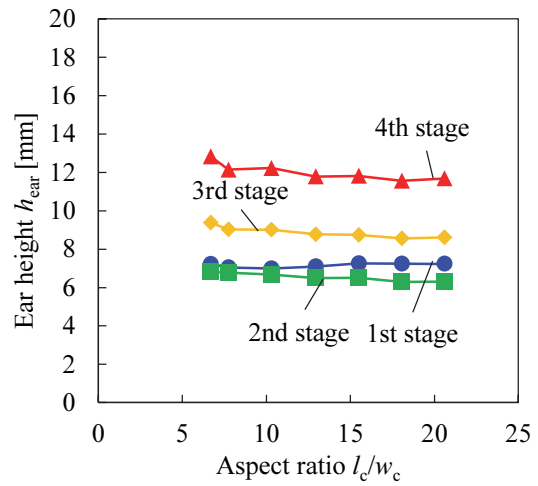


Figure 17: Effect of blank corner length r_{1b} on ear height h_{ear} after each stage ($\alpha=0.54, \beta=1.72$)

4 CONCLUSIONS

- This paper presents the effects of the blank shape, such as the longitudinal length and the corner shape, on the four-stage deep drawing for forming the flat and deep rectangular cup, which the aspect ratio of the cross section is extremely high.
- The blank shape was the rectangle of which the length and the width are l_b and w_b , and the corner shape is elliptic arc of which the longitudinal and the width length are r_{1b} and r_{wb} . The effect of l_b and r_{1b} on the thickness and the ear height was investigated by the finite element analysis in this study.
- The local thinning and the large ear occurred when the blank length l_b was too large,

or the corner length r_{1b} was too small. On the other hand, the edge side height became low and the folding occurred when the blank length l_b was too short, or the corner length r_{1b} was too large.

- The optimum blank length l_b was determined as the distance between the blank end the fourth die hole end in the longitudinal direction was 0.54 times of that in the width direction. The optimum corner length r_{1b} in the longitudinal direction was 1.72 times of the corner length r_{wb} in the width direction.
- The effect of the aspect ratio of the case cross section on the formability was small under the condition that the aspect ratio was 6.7~20.6. Therefore, the optimized blank could be applied for forming the flat rectangular case with various aspect ratio.

REFERENCES

- [1] Koga, N., Jiang, W., Kageyama, J. and Suzuki, T. Shape precision improvement of impact extruded 3003 aluminum alloy square cups by means of ironing. *Journal of The Japan Institute of Light Metals* (2013) **63** (3), 106-110 (in Japanese).
- [2] Hatanaka, N., Waki, S. and Iizuka T. Deep drawing of square cup with airtight using developed blank of aluminum sheet in combination with friction stir welding. *Journal of The Japan Institute of Light Metals* (2015), **65** (3), 79-85 (in Japanese).
- [3] Sachs, G., 1951. *Principles and Methods of Sheet-Metal Fabricating* (1951), Reinhold Publishing Corporation.
- [4] Ahmetoglu, M., Broek, T.R., Kinzel, G. and Altan, T. Control of Blank Holder Force to Eliminate Wrinkling and Fracture in Deep-Drawing Rectangular Parts. *CIRP Annals* (1995) **44/1**, 247-250.
- [5] Osakada, K., Wang, C.C. and Mori, K. Controlled FEM simulation for determining history of blank holding force in deep drawing. *CIRP Annals* (1995) **44/1**, 243-246.
- [6] Pegada, V., Chun, Y. and Santhanam, S. An algorithm for determining the optimal blank shape for the deep drawing of aluminum cups. *Journal of Materials Processing Technology* (2002) **125-126**, 743-750.